Pushing the thickness limit of the giant Rashba effect in ferroelectric semiconductor GeTe

Boris Croes, Alexandre Llopez, Calvin Tagne-Kaegom, Bodry Tegomo Chiogo, Bertrand Kierren, Pierre Müller, Stefano Curiotto, Patrick Le Fèvre, François Bertran, Andrés Saúl, et al.

Pushing the thickness limit of the giant Rashba effect in ferroelectric semiconductor GeTe

Boris Croes,[†,§] Alexandre Llopez,[†] Calvin Tagne-Kaegom,[‡] Bodry Tegomo-Chiogo,[‡] Bertrand Kierren,[‡] Pierre Müller,[†] Stefano Curiotto,[†] Patrick Le Fèvre,[¶,‖] François Bertran,[¶] Andrés Saùl,[†] Yannick Fagot-Revurat,[‡] Frédéric Leroy,[†] and Fabien Cheynis[*,†]

†*Aix Marseille Univ, CNRS, CINAM, AMUtech, 13288 Marseille, France*

‡*Institut Jean Lamour, UMR 7198, CNRS-Université de Lorraine, Campus ARTEM, 2 allée André Guinier, BP 50840, 54011 Nancy, France*

¶*Université Paris-Saclay, Synchrotron SOLEIL, L'Orme des Merisiers, Départementale 128, 91190 Saint-Aubin, France*

§*Current address: Université de Strasbourg, CNRS, IPCMS, UMR 7504, Strasbourg 67000, France*

‖*Univ Rennes, IPR - UMR 6251, CNRS, Rennes F-35000, France*

E-mail: fabien.cheynis@univ-amu.fr

Abstract

Ferroelectric Rashba semiconductors (FERSCs) such as α-GeTe are promising candidates for energy-efficient information technologies exploiting spin-orbit coupling (SOC) and termed spin-orbitronics. In this work, the thickness limit of the Rashba-SOC effect in α-GeTe films is investigated. We demonstrate, using angle-resolved photoemission

spectroscopy (ARPES) and first-principles calculations performed on pristine GeTe, that down to 1 nm, GeTe(111) films on Sb-covered Si(111) substrate continuously exhibit a giant Rashba effect characterized, at 1 nm, by a constant of 5.2±0.5 eV.Å. X-ray photoemission spectroscopy (XPS) allow understanding the persistence of the Rashba effect by evidencing a compensation of Ge vacancy defects resulting form the insertion of Sb interfacial atoms in the early-stage growth of the GeTe(111) films.

Keywords

Ferroelectric Rashba Semiconductors, GeTe, Rashba spin-texture, quantum well, transport properties, size effect

The most recent developments of spintronics, termed spin-orbitronics, use the functionalities of the spin-orbit coupling (SOC) to manipulate charge carrier spins. In this context, the emergent ferroelectric Rashba semiconductors (FERSCs) displaying a large spin-orbit coupling stand out as versatile platforms for the realization of low-power all-electric controlled spintronic devices. FERSC GeTe in its α-phase ($R3m$ space group) has been intensively studied over the last decade owing to a voltage-controllable Rashba spin-orbit coupling [1] and spin texture of the electronic band structure [2,3] along with a non reciprocal charge transport [4] and a switchable spin-to-charge conversion at room-temperature. [5] This quantum material has also been investigated for its thermoelectric properties [6] and has been predicted to allow for terahertz detection owing to its inversion-symmetry breaking. [7] At the fundamental level, the electronic band structure of GeTe(111) has been determined on thin films [2–4,8–13] and crystals. [14] In all cases, GeTe is characterized by a giant Rashba spin-splitting of the band structure as quantified by a Rashba constant among the highest reported values ($\simeq 4.5$ eV.Å along the Γ - K direction of the reciprocal space).

To date, the influence of the substrate on the electronic band structure at the origin of the demonstrated macroscopic properties has been overlooked as previous reports focused on bulk-like films (≥ 20 nm). This is of particular significance in the context of applications

where miniaturization is pursued. To the best of our knowledge, Reference 12 is the only report on the thickness-dependence of the band structure of GeTe on Si(111) substrates. The authors derived a thickness limit of 2.1 ± 0.5 nm below which the bulk giant Rashba effect ceased to exist in GeTe(111) films. In the current work, we characterize the evolution of the Rashba effect in GeTe thin-films on a modified Si(111) substrate, namely Si(111)-$\sqrt{3}\times\sqrt{3}$-Sb reconstructed surface (Si(111)-Sb) using X-ray photoemission spectroscopy (XPS) and angle-resolved photoemission spectroscopy (ARPES). We establish that GeTe/Si(111)-Sb films as thin as 1 nm still exhibit a giant spin splitting of the band structure characterized by a Rashba constant of 5.2 ± 0.5 eV.Å in agreement with first-principle calculations performed on pristine GeTe(111). The contribution of interfacial Sb on epitaxial growth and the resulting band structure is investigated. We conclude that interfacial Sb helps to reveal intrinsic GeTe properties by compensating Ge vacancies otherwise present in the early-stage growth. These results suggest to reconsider the thickness limits of fundamental properties such as Rashba effect and ferroelectricity in the context of spin-orbitronics applications.

Electronic band structure determination of GeTe(111) has generated an impressive research effort over the last decade. A non-exhaustive list of previous studies include GeTe crystals[14] and thin films elaborated on various substrates such as Si(111),[3,12] Si(111)-Sb,[8] BaF_2,[9,10,13] InP(111)[2,11] and Al_2O_3(0001).[4] Despite being well established and corroborated by first principle calculations, the thickness-dependence of the band structure of GeTe(111) films has been only reported in Reference.[12]

In a recent study, we have investigated the growth properties of ultrathin GeTe(111) films (0.1-4 nm) deposited by MBE on Sb-covered Si(111).[15] It is established that this approach improves the crystalline quality of GeTe(111) films from the early-stage growth (see Ref. 16 and Supporting Information Section 1 for STM images of 1 nm- and 2 nm-GeTe films) as opposed to standard Si(111).[12,17] The influence of Sb on the electronic band structure down the ultrathin regime remains however to be investigated.

In the current work, we perform the band structure determination of GeTe/Si(111)-Sb

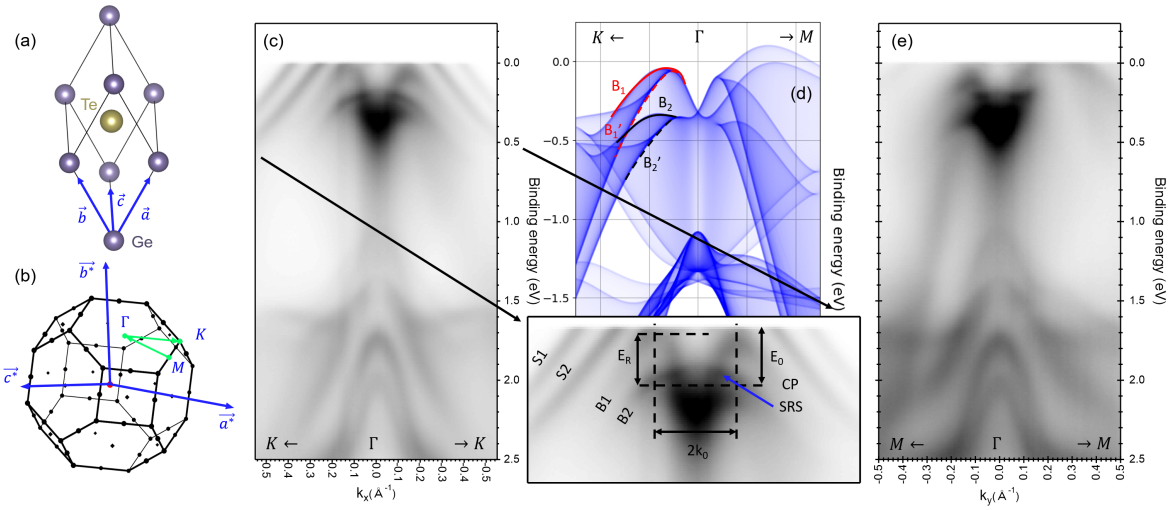

Figure 1: (a) α-GeTe rhombohedral unit cell ($R3m$ space group) and (b) Brillouin zone with high-symmetry points of the (111) lattice plane. Bulk band structure of a 400 nm-thick α-GeTe determined by ARPES in the (c) K-Γ-K, (e) M-Γ-M directions and (d) by DFT calculation in the K-Γ-M directions (see text for details on DFT calculations).

films in the 1-400 nm thickness range using ARPES technique and compare experimental results with first-principle calculations including spin-orbit coupling on pristine GeTe films. DFT calculations have been performed using Quantum Espresso code[18,19] and the Perdew Burke Ernzerhof (PBE) ansatz[20] with fully relativistic ultrasoft pseudopotentials from the PSlibrary.[21] Details are available in Supporting Information Section 2 for DFT calculations and Section 3 for XPS - ARPES measurements. Figure 1 depicts the bulk real and reciprocal lattices along with the electronic band structure of α-GeTe in the high-symmetry K-Γ-M directions. DFT band structure of bulk GeTe has been determined by superposing dispersion bands obtained at k_z-points equally-spaced along the reciprocal direction of the growth axis. The envelope corresponds to the bulk band structure independently of potential effects resulting from transition matrix elements. Close to the Fermi level, the dispersion relation is characterized by two surface states, usually labelled S1 and S2 (see the inset of Figure 1c) and two bulk states (B1 and B2). These four states originating from two orbital bands that are degeneracy-lifted by spin-orbit coupling are responsible for metal-like properties. Magnetotransport measurements indeed confirm that GeTe(111) films conduct as a heavily

p-doped narrow-gap semiconductor (see Supporting Information Figure S4 for temperature-dependent resistivity, charge carrier density and hole mobility measurements) in agreement with previous studies.[4–6,22,23] As only B1/B2 states are fully occupied in GeTe(111) films, we will, here, focus on the Rashba effect in bulk bands. Close to the bulk band CP (see the inset of Figure 1c at BE $\simeq$ 0.35 eV) a surface-induced resonant state (SRS) is also visible. Along the M-Γ-M direction (Figure 1e), surface states are usually less intense and bulk bands appear steeper. We observe an asymmetry in the ARPES intensity in the bulk states for $k_y > 0$ or $k_y < 0$. despite the use of a linearly-polarized light probing both in-plane and out-of-plane orbitals (p-polarization). Crystalline three-fold symmetry of bulk α-GeTe is likely to be responsible of this effect although geometry dependence of the photoemission matrix elements cannot be excluded.

First-principle calculations allow us to further identify the chemical and orbital nature of the electronic bands. In materials such as α-GeTe, SOC mixes spin and orbital degrees of freedom so that electronic states are described by their total angular momentum $\vec{J} = \vec{L} + \vec{S}$ as summarized in Ref. 10. For simplicity, we focus our analysis on the envelope of the bulk band structure shown in Figure 1d. Figure 2 decomposes GeTe(111) bands close to the Fermi level according to their chemical (Ge vs Te) and orbital origin (S, $P_{1/2}$ or $P_{3/2}$). Above the Fermi level, bulk states are related to Ge atoms while, below the Fermi level, electronic band structure is clearly dominated by the contribution of Te atoms except (i) in the direct vicinity of the crossing point located at Γ and (ii) in the $\Gamma - M$ direction ($k_x \simeq$-0.35 Å^{-1}) where B1/B2 states originate almost equally from Ge and Te atoms (Figure 2a). More specifically, above the Fermi level, Te-dominated S orbitals are exceeded by Ge-dominated $P_{1/2}$ and $P_{3/2}$ orbitals. Below the Fermi level, S orbitals contribution to B1/B2 bulk states are related to Ge atoms while $P_{3/2}$ orbitals contribution mostly originate from Te atoms. $P_{1/2}$ orbitals show a k_x-dependent chemical contribution that results in the partial compensations observed in the total DOS. These results are in agreement with DFT calculations reported in Ref. 10.

When decreasing GeTe(111)/Si(111)-Sb thickness down to $\simeq$ 5 nm, the aforementioned

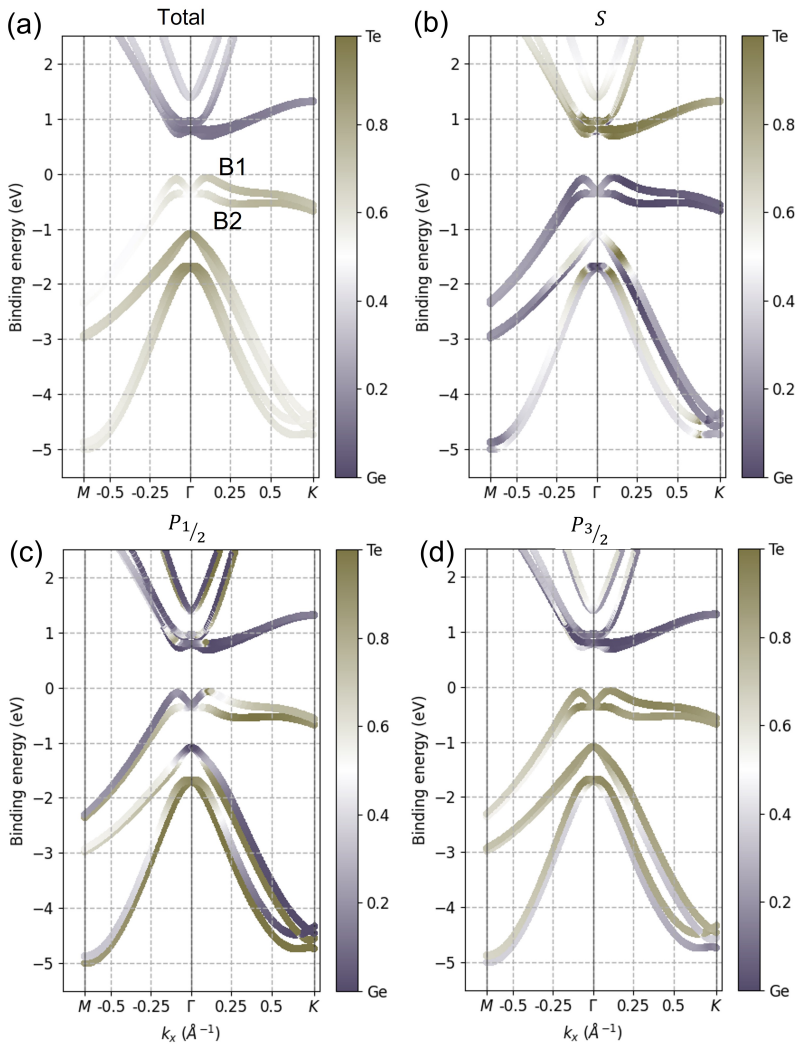

Figure 2: DFT calculations of α-GeTe k-resolved density of states (DOS) projected on the atomic orbitals indexed by their total angular momentum $\vec{J}$. In each case, the color codes for the chemical nature of a given state and the width of the bands equals the contribution of this state to the total DOS. (a) Total density of state. Contributions of (b) S, (c) $P_{1/2}$ and (d) $P_{3/2}$ orbitals to the total DOS.

band structure remains qualitatively unaffected except the electron-like continuum (1.5 eV $\leq$ BE $\leq$ 0.5 eV) that now shows discrete bands due to a reduction of the lattice unit number in the vertical direction also called quantum well (QW) effect (see black arrow in Figure 3a). Theoretical calculations superposed to the second derivative of the experimental band structures also predict the reduction of band number in the continuum with the film thickness (Figure 3e-h). Interestingly, QW states intersections with SRS and CP points may show

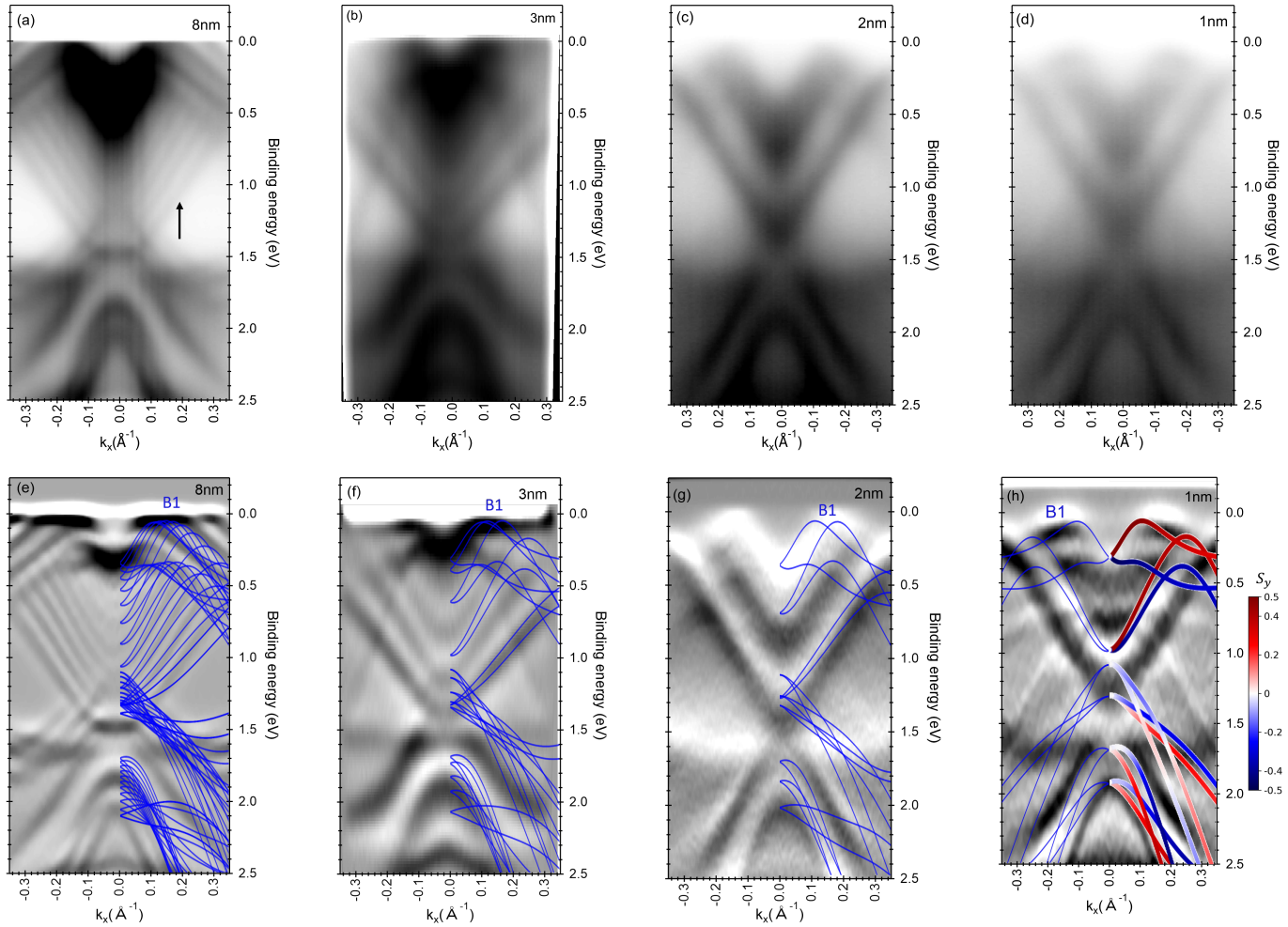

Figure 3: GeTe/Si(111)-Sb band structure determined by ARPES as a function of the film thickness (Γ-K direction, $h\nu$=25 eV, T=20 K): (a) 8 nm, (b) 3 nm, (c) 2 nm, (d) 1 nm. (e-h) Respective second-order derivatives and DFT calculations of the experimental band structures.

surface-driven non trivial topology as reported for bulk states in α-GeTe.[24]

Below 5 nm (Figure 3b-d), surface bands (S1/S2) vanish and bulk bands (B1/B2) appear broader. Apparent similarities of Figure 3g-h probably result in part from sample thickness distribution (see Fig. S1). However, the disappearance of the QW state with a crossing point close to BE$\simeq$ 0.7 eV in Figure 3h confirms the mean thickness decrease between both samples. B1/B2 maxima remain also clearly visible and located at a wavevector ($k_x \simeq 0.1 - 0.2\,\text{Å}^{-1}$) and a binding energy ($E_\text{b} \simeq E_\text{F}$) that differs from CP. This suggests the persistence of a spin-

orbit splitting of the electronic bands for GeTe/Si(111)-Sb even in the ultra-low thickness regime. A question remains concerning the continuation of the spin texture of the electronic band structure in this thickness regime. Expectation values of the spin components have been determined by first-principle calculations. Figure 3h shows in red-blue color code the spin component S_y on a $\Gamma - \mathrm{K}$ path oriented along k_x for a 1 nm-GeTe film (see Figure S2 of Supporting Information for a complete spin component characterization). It confirms that bands close to the Fermi level are still spin polarized with a strong in-plane component as predicted in bulk GeTe in Ref. 1 and later confirmed experimentally.[8,9,25]

We now quantitatively assess the Rashba spin-orbit coupling in experimental and calculated band structures. From a general standpoint, the Rashba-effect dispersion relation can be expressed in the vicinity of an orbital band extremum as:

$$E_{\pm}(\mathbf{k}) = \frac{\hbar^2 \mathbf{k}^2}{2m^\star} \pm \alpha_{\mathrm{R}} |\mathbf{k}| + E_0 = \frac{\hbar^2 (\mathbf{k} \pm \mathbf{k_0})^2}{2m^\star} + E_{\mathrm{R}} \quad (1)$$

where $\hbar$ is the reduced Planck constant, $\mathbf{k}$ is the carrier wave vector, $m^\star$ is the carrier effective mass, α_{R} is the so-called Rashba constant, E_0 is the binding energy of the band crossing point and $\mathbf{k_0}$ (resp. E_{R}) defines the position in wave vector (resp. energy) of the spin-split extrema (see Figure 1c for graphical definitions). Both α_{R} and $m^\star$, which can be determined from ARPES measurements ($\alpha_{\mathrm{R}} = 2E_{\mathrm{R}}/k_0$ and $m^\star = \hbar^2 k_0^2 / 2E_{\mathrm{R}}$). α_{R} quantifies the Rashba spin-splitting of the electronic bands and both α_{R} and $m^\star$ are involved in the electronic (spin-)transport properties of the material.

Figure 4 summarizes the evolution of the Rashba and $m^\star$ parameters with respect to GeTe film thicknesses as determined from ARPES experiments and DFT calculations (see Figure S3 of Supporting Information for data on E_{R} and k_0). Effective carrier mass remains constant throughout the covered thickness range ($m^\star \simeq 0.19\,\mathrm{m_e}$) which lies between values from the literature for GeTe effective mass determined from ARPES measurements.[1,12] However, we do not evidence an increase of the effective mass below 10 nm as reported in Ref. 12.

For thick films (i.e. ≥ 10 nm), we measure a Rashba constant in the Γ-K direction of

4.8±0.3 eV.Å in quantitative agreement with the DFT calculations and previous reports. In their recent work,[12] X. Yang *et al.* reported a reduction of the Rashba constant by a factor $\simeq$ 2 (2.12 eV.Å) for 5 nm-GeTe films on Si(111) before the band splitting disappearance below a critical thickness of 2.1±0.5 nm. The authors attribute this decrease to a decline of the ferroelectric polarization and Berry curvature induced by a transition from space group $R3m$ to higher symmetry $R\bar{3}m$ space group at low GeTe thicknesses. We do not observe this evolution in the GeTe/Si(111)-Sb system: 5 nm-GeTe films on Si(111)-Sb still show a giant Rashba constant of 4.1±0.3 eV.Å. More interestingly, in the ultrathin regime (1-3 nm), the Rashba-split band structure is preserved in GeTe/Si(111)-Sb films with a measured Rashba constant for a 1 nm film of 5.2±0.5 eV.Å. Owing to the experimental uncertainties, we cannot undoubtedly conclude on an increase of the Rashba effect even though Figure 4 would suggest. DFT calculations performed on pristine GeTe slabs also confirm that the giant Rashba effect in GeTe(111) is maintained down to 1 nm. Our combined experimental and theoretical data thus clearly demonstrate that a giant Rashba effect still occurs in 1-5 nm-GeTe/Si(111)-Sb films as long as the inversion symmetry breaking of the primitive GeTe unit cell is preserved. This opens new perspective on thickness limits of both ferroelectricity- and Rashba-based spintronics. The specific role of interfacial Sb on the GeTe electronic band structure will be now investigated.

In a previous paper, we have studied the morphology and structure of GeTe films deposited on Si(111)-Sb in the ultrathin regime (0.1-4 nm).[15] The improved crystalline quality of GeTe(111) ultrathin films on Si(111)-Sb with respect to Si(111) substrate has been attributed to a surfactant effect of Sb that allows for a complete elastic stress relaxation of Ge deposited layers by facilitating the introduction of interfacial misfit dislocations.[26–29] Let us note that other elements such as Mn,[30] Fe,[31] Cu,[6] Pb[32] have been also reported to diffuse into GeTe.

The role played by Sb in ultrathin GeTe(111) films on Si(111)-Sb still needs to be scrutinized from chemical and band structure perspectives. XPS measurements obtained on

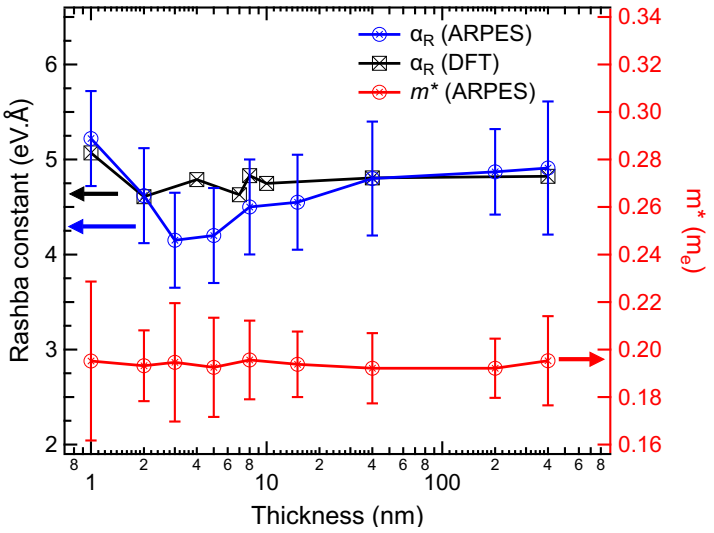

Figure 4: Rashba constant α_R (blue) and hole effective mass $m^\star$ (red) of GeTe films on Si(111)-Sb as a function of the film thickness determined by ARPES measurements and DFT calculations.

GeTe(111)/Si(111)-Sb films of different thicknesses (1-400 nm) are shown in Figure 5. Bulk-like behaviour of GeTe films on Si(111)-Sb is illustrated in Figure 5a showing the XPS spectrum obtained for a 400 nm-thick film in the [24−44 eV] binding energy window where both Te 4*d* and Ge 3*d* levels are observed. For both Te and Ge levels, two doublets are required to adequately fit experimental data. Doublets at higher binding energies ($BE_{Te,4d,3/2} = 41.5$ eV, $BE_{Te,4d,5/2} = 40.03$ eV and $BE_{Ge,3d,3/2}$= 29.98 eV, $BE_{Ge,3d,5/2} = 29.43$ eV) are identified as bulk contributions while doublets at lower binding energies ($BE_{Te,4d,3/2} = 41.03$ eV, $BE_{Te,4d,5/2} = 39.58$ eV and $BE_{Ge,3d,3/2} = 29.53$ eV, $BE_{Ge,3d,5/2} = 28.98$ eV) are attributed to surface contributions.[3] We assign the small shoulder close to BE = 32.5 eV to oxidized states of Ge[33] probably resulting from oxygen diffusion through the Te-capping layer. This contribution remains negligible compared to principal components. Ultrathin films have been protected from oxygen by being transported to the beamline setup using a custom-made UHV suitcase. Large-scale XPS surveys showed no Sb-related signal in thick films. From the component areas, the stoichiometry of bulk-like GeTe(111) films on Si(111)-Sb can be derived to be $Ge_{0.46\pm0.02}Te_{0.54\pm0.02}$ in excellent agreement with reported values with a Ge vacancy content

of $\sim 10\,\%$.[34,35]

For GeTe films thinner than 5 nm, the Te atomic content as determined solely from Te 4*d* and Ge 3*d* contributions surprisingly increases from 56.4 % to 79.2 % (Figure 5b). A closer examination of the XPS spectra of ultrathin films allows to identify two growing peaks centered around BE = 32 eV (Figure 5c). The appearance of a doublet in wider XPS surveys (not shown) at BE = 532 eV and BE = 527 eV rules out an O-related origin of this new component. O 1*s* level is indeed not spin-split. This additional contribution can be thus safely attributed to Sb 4*d* levels. By increasing, on a 2 nm-thick GeTe film, the photoelectron angle from 0 ° to 30 ° with respect to the film normal direction to enhance surface sensitivity, we have evidenced an increasing Sb 3*d* contribution with respect to the Te 3*d* signal.[15] It can be concluded that Sb atoms act as surfactant on the film surface during the growth process. The decrease of Sb 4*d* contribution for thicker films observed in Figure 5 additionally shows that Sb atoms are progressively incorporated in GeTe to become negligible above 5 nm. Simple geometrical calculations derived in Supporting Information Section 3 corroborates that Sb surfactant atoms are progressively incorporated in the GeTe film and compensate Ge bulk vacancies up to 5 nm where all the Sb atoms available at the film/substrate interface are incorporated. Reference 22 also supports our conclusions as Ge substitution by Sb in GeTe crystals has been described as a textbook solid solution for similar compositions.

To go one step further in our analysis of the system, we decompose XPS spectra by including Sb element in the Ge and Te components. The surface, bulk and total contributions of all elements in ultrathin GeTe films are presented in Figure 5d. Sb atomic concentration decreases linearly with the film thickness. Sb atoms are homogeneously distributed in the film as surface and bulk contributions follow quantitatively the same evolution. Te atomic concentration slowly decreases with the film thickness with a more significant Te-enrichment at the film surface for ultrathin films. Ge atomic depletion recovers regularly as the film thickness increases. Interestingly, Ge and Sb concentrations add up to reach a value of $40 \pm 2\,\%$ for ultrathin films close to the bulk content of $Ge_{0.46\pm0.02}Te_{0.54\pm0.02}$. This trend

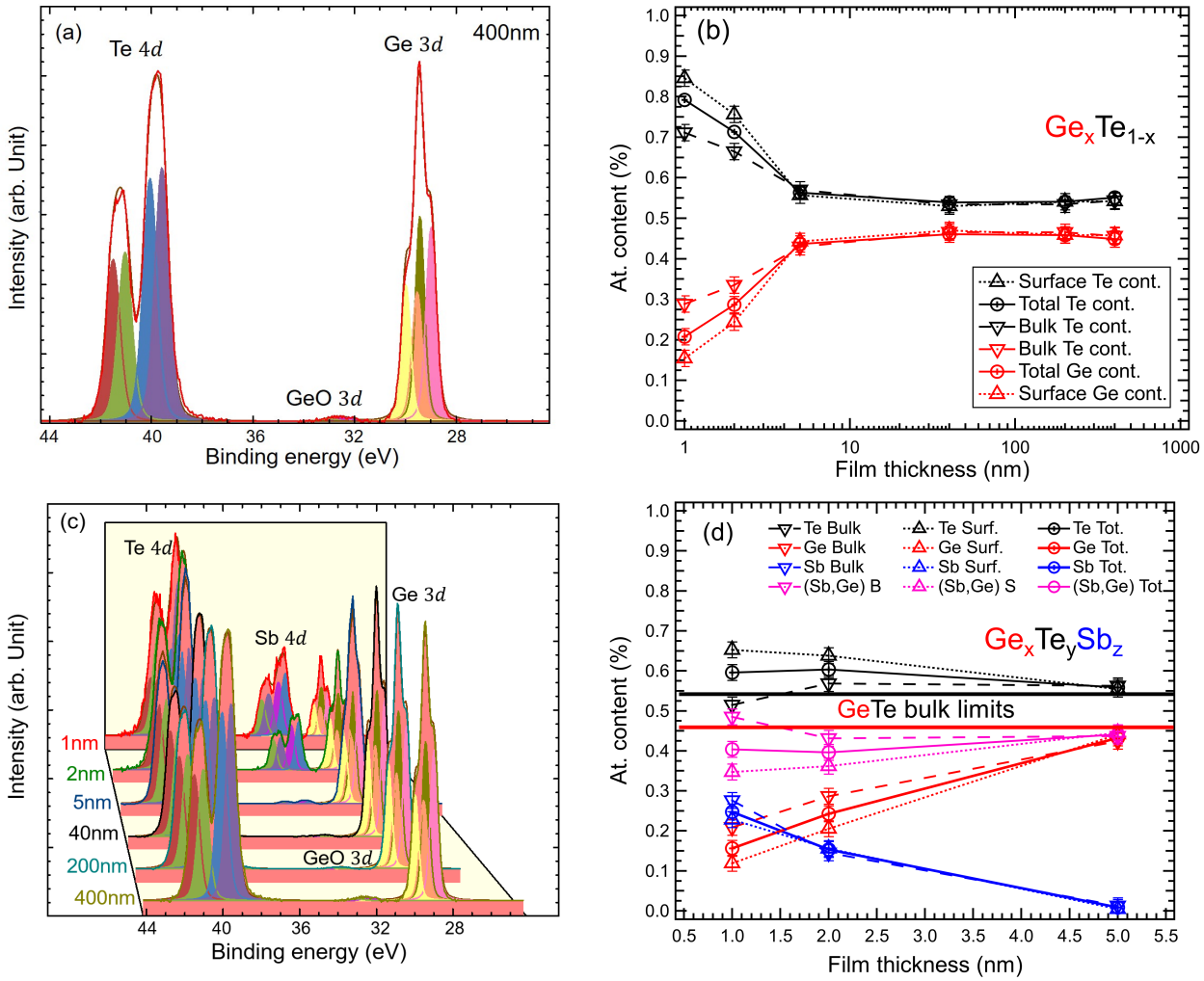

Figure 5: XPS measurements of GeTe(111) thin films ($h\nu$ =800 eV, T=20 K). (a) Spectrum decomposition of the Te 4d, Sb 4d and Ge 3d levels for a 400 nm-thick film. For each element, two spin-split doublets are used to fit experimental data: a bulk (resp. surface) contribution at high (resp. low) binding energy. (b) GeTe film stoichiometry determined from the XPS spectra decomposition as a function of the film thickness. (c) Evolution of the XPS spectra as a function of the film thickness. (d) Evolution of the Sb 4d contribution to the $Ge_xTe_ySb_z$ system for GeTe film thicknesses below 5 nm.

is enhanced when considering only the bulk components of the 1 nm-GeTe film where a stoichiometric $(Ge,Sb)_{0.49\pm0.02}Te_{0.51\pm0.02}$ is reached. From our observations, we can thus conclude that Sb atoms that are easily incorporated in GeTe films[15] diffuse to the surface to compensate the Te over-stoichiometry evidenced in Figure 5d. We could, here, wonder about the potential occurrence of a well-defined chemical phase mixing these three elements (*e. g.* $Ge_2Sb_2Te_5$, GST). Refs. 36,37 have however excluded the formation of a GST phase in the ultrathin regime. The authors concluded that GeTe films were energetically favored on Si(111)-Sb substrates by the tendency of Sb atoms to form resonant bonds, that are also involved in the stabilization of the non-centrosymmetric α-GeTe phase. In other words, by keeping Ge vacancy level close to the GeTe bulk limit and reducing Te surface fraction, random interdiffusion of Sb interfacial layer facilitates GeTe epitaxial growth in the early stage and helps maintaining the intrinsic electronic properties of α-GeTe down to 1 nm.

Finally let us note that the Te 4*d* and Ge 5*d* levels reported in Table T1 (see Supporting Information Section 3) progressively shift toward lower binding energies when the film thickness is reduced. It seems contradictory to the *n*-type doping of Sb in GeTe films reported in References 22,38. Beyond possible band-bending effects, we hypothesize that Ge defect concentration at the interface is significantly higher than in bulk-GeTe and cannot be entirely compensated by Sb substitution. When considering this plausible uncompensated interfacial Ge defects and the apparent increase of the Rashba constant below 3 nm, we tentatively anticipate a Rashba effect enhancement in ultrathin Sb-doped GeTe films. This is supported by the increase of the thermoelectric properties of Sb-doped GeTe crystals with a maximum reached for a Sb content of $\simeq 5-10\,\%$.[6,22,38]

To summarize, we have characterized the evolution of the electronic band structure of GeTe(111) films deposited on Si(111)-Sb as a function of the layer thickness down to 1 nm using XPS and ARPES techniques. DFT calculations allow us to continuously follow and understand the band dispersion details (*i.e.* band morphology and chemical/orbital origin). Fundamental quantities such as Rashba constant and carrier effective mass have been de-

termined from experiments and simulations. Our results demonstrate that 1 nm-thick GeTe films on Si(111)-Sb still exhibit a giant Rashba effect with a Rashba constant of 5.2 ± 0.5 eV.Å. The influence of interfacial Sb on the electronic properties has been investigated. By compensating Ge vacancies, Sb substitution favours epitaxy from the early stages and allows to maintain intrinsic GeTe electronic properties. Sb is progressively incorporated in GeTe and is not detected above 5 nm. Our results suggest that Rashba effect could be even reinforced by intentionally doping GeTe films at 5-10 %-Sb in the ultrathin regime.

Acknowledgement

The project leading to this publication has received funding from Excellence Initiative of Aix-Marseille University A*MIDEX, a French Investissements d'Avenir program (AMX-22-RE-AB-043) and through the AMUtech Institute. This work has also been supported by the ANR grant FETh (Grant No. ANR-22-CE08-0023). We thank Frédéric Bedu and Igor Ozerov (CINaM\PLANETE platform) for their help in the fabrication of Hall devices. We also thank Khaled Alkema and Birame Diakhate for their contribution during their respective MSc internship.

Supporting Information Available

The following file is available free of charge.

- Supporting Information.pdf: Additional information on the surface morphology of ultrathin GeTe films, ARPES measurements analysis and magnetotransport measurements.

References

(1) Di Sante, D.; Barone, P.; Bertacco, R.; Picozzi, S. Electric Control of the Giant Rashba Effect in Bulk GeTe. *Adv. Mater.* **2013**, *25*, 509–513.

(2) Krempaský, J.; Muff, S.; Minár, J.; Pilet, N.; Fanciulli, M.; Weber, A. P.; Guedes, E. B.; Caputo, M.; Müller, E.; Volobuev, V. V.; Gmitra, M.; Vaz, C. A. F.; Scagnoli, V.; Springholz, G.; Dil, J. H. *Operando* Imaging of All-Electric Spin Texture Manipulation in Ferroelectric and Multiferroic Rashba Semiconductors. *Phys. Rev. X* **2018**, *8*, 021067.

(3) Rinaldi, C.; Varotto, S.; Asa, M.; Sławińska, J.; Fujii, J.; Vinai, G.; Cecchi, S.; Di Sante, D.; Calarco, R.; Vobornik, I.; Panaccione, G.; Picozzi, S.; Bertacco, R. Ferroelectric Control of the Spin Texture in GeTe. *Nano Lett.* **2018**, *18*, 2751–2758.

(4) Li, Y.; Li, Y.; Li, P.; Fang, B.; Yang, X.; Wen, Y.; Zheng, D.-x.; Zhang, C.-h.; He, X.; Manchon, A.; Cheng, Z.-H.; Zhang, X.-x. Nonreciprocal Charge Transport up to Room Temperature in Bulk Rashba Semiconductor α-GeTe. *Nat Commun* **2021**, *12*, 540.

(5) Varotto, S. et al. Room-Temperature Ferroelectric Switching of Spin-to-Charge Conversion in Germanium Telluride. *Nat Electron* **2021**, *4*, 740–747.

(6) Fan, Y.; Xie, C.; Zhang, T.; Yang, X.; Chen, Z.; Tang, X.; Tan, G. Contrasting the Roles of Cu Interstitials and Sb Substitutions in Regulating Ferroelectric Distortions and Thermoelectric Properties of α-GeTe. *ACS Appl. Energy Mater.* **2023**, *6*, 4065–4071.

(7) Zhang, Y.; Fu, L. Terahertz Detection Based on Nonlinear Hall Effect without Magnetic Field. *Proc. Natl. Acad. Sci.* **2021**, *118*, e2100736118.

(8) Liebmann, M. et al. Giant Rashba-Type Spin Splitting in Ferroelectric GeTe(111). *Adv. Mater.* **2016**, *28*, 560–565.

(9) Krempaský, J. et al. Disentangling Bulk and Surface Rashba Effects in Ferroelectric α -GeTe. *Phys. Rev. B* **2016**, *94*, 205111.

(10) Krempaský, J.; Fanciulli, M.; Nicolaï, L.; Minár, J.; Volfová, H.; Caha, O.; Volobuev, V. V.; Sánchez-Barriga, J.; Gmitra, M.; Yaji, K.; Kuroda, K.; Shin, S.; Komori, F.; Springholz, G.; Dil, J. H. Fully Spin-Polarized Bulk States in Ferroelectric GeTe. *Phys. Rev. Research* **2020**, *2*, 013107.

(11) Kremer, G.; Jaouen, T.; Salzmann, B.; Nicolaï, L.; Rumo, M.; Nicholson, C. W.; Hildebrand, B.; Dil, J. H.; Minár, J.; Springholz, G.; Krempaský, J.; Monney, C. Unveiling the Complete Dispersion of the Giant Rashba Split Surface States of Ferroelectric $\ensuremath{\alpha}\text{\ensuremath{-}}\mathrm{GeTe}(111)$ by Alkali Doping. *Phys. Rev. Res.* **2020**, *2*, 033115.

(12) Yang, X.; Li, X.-M.; Li, Y.; Li, Y.; Sun, R.; Liu, J.-N.; Bai, X.; Li, N.; Xie, Z.-K.; Su, L.; Gong, Z.-Z.; Zhang, X.-Q.; He, W.; Cheng, Z. Three-Dimensional Limit of Bulk Rashba Effect in Ferroelectric Semiconductor GeTe. *Nano Lett.* **2021**, *21*, 77–83.

(13) Clark, O. J.; Wadgaonkar, I.; Freyse, F.; Springholz, G.; Battiato, M.; Sánchez-Barriga, J. Ultrafast Thermalization Pathways of Excited Bulk and Surface States in the Ferroelectric Rashba Semiconductor GeTe. *Advanced Materials* **2022**, *34*, 2200323.

(14) Ryu, H.; Lihm, J.-M.; Cha, J.; Kim, B.; Kim, B. S.; Kyung, W.; Song, I.; Kim, Y.; Han, G.; Denlinger, J.; Chung, I.; Park, C.-H.; Park, S. R.; Kim, C. Chemical Control of the Rashba Spin Splitting Size of α-GeTe(111) Surface States by Adjusting the Potential at the Topmost Atomic Layer. *Phys. Rev. B* **2021**, *103*, 245113.

(15) Croes, B.; Cheynis, F.; Fagot-Revurat, Y.; Müller, P.; Curiotto, S.; Leroy, F. Early-Stage Growth of GeTe on Si(111)-Sb. *Phys. Rev. Materials* **2023**, *7*, 014409.

(16) Wang, R.; Boschker, J. E.; Bruyer, E.; Di Sante, D.; Picozzi, S.; Perumal, K.; Gius-

sani, A.; Riechert, H.; Calarco, R. Toward Truly Single Crystalline GeTe Films: The Relevance of the Substrate Surface. *J. Phys. Chem. C* **2014**, *118*, 29724–29730.

(17) Giussani, A.; Perumal, K.; Hanke, M.; Rodenbach, P.; Riechert, H.; Calarco, R. On the Epitaxy of Germanium Telluride Thin Films on Silicon Substrates. *Phys. Status Solidi B* **2012**, *249*, 1939–1944.

(18) Giannozzi, P. et al. QUANTUM ESPRESSO: A Modular and Open-Source Software Project for Quantum Simulations of Materials. *J. Phys.: Condens. Matter* **2009**, *21*, 395502.

(19) Giannozzi, P. et al. Advanced Capabilities for Materials Modelling with Quantum ESPRESSO. *J. Phys.: Condens. Matter* **2017**, *29*, 465901.

(20) Perdew, J. P.; Burke, K.; Ernzerhof, M. Generalized Gradient Approximation Made Simple. *Phys. Rev. Lett.* **1996**, *77*, 3865–3868.

(21) Dal Corso, A. Pseudopotentials Periodic Table: From H to Pu. *Computational Materials Science* **2014**, *95*, 337–350.

(22) Levin, E. M. Effects of Ge Substitution in GeTe by Ag or Sb on the Seebeck Coefficient and Carrier Concentration Derived from Te 125 NMR. *Phys. Rev. B* **2016**, *93*, 045209.

(23) Zhu, C.; Luo, F.; Wang, J.; He, X.; Yang, Z.; Zhang, S.; Wang, J.; Liu, H.; Sun, Z. Synthesis Mechanism and Magnetoresistance Effect of Millimeter-Sized GeTe Faceted Crystals. *Journal of Physics and Chemistry of Solids* **2022**, *165*, 110671.

(24) Krempaský, J.; Nicolaï, L.; Gmitra, M.; Chen, H.; Fanciulli, M.; Guedes, E. B.; Caputo, M.; Radović, M.; Volobuev, V. V.; Caha, O.; Springholz, G.; Minár, J.; Dil, J. H. Triple-Point Fermions in Ferroelectric GeTe. *Phys. Rev. Lett.* **2021**, *126*, 206403.

(25) Elmers, H. J. et al. Spin Mapping of Surface and Bulk Rashba States in Ferroelectric α -GeTe(111) Films. *Phys. Rev. B* **2016**, *94*, 201403.

(26) Voigtländer, B.; Zinner, A. Surfactant-mediated Epitaxy of Ge on Si(111): The Role of Kinetics and Characterization of the Ge Layers. *Journal of Vacuum Science & Technology A: Vacuum, Surfaces, and Films* **1994**, *12*, 1932–1937.

(27) Meyer, G.; Voigtländer, B.; Amer, N. M. Scanning Tunneling Microscopy of Surfactant-Mediated Epitaxy of Ge on Si(111): Strain Relief Mechanisms and Growth Kinetics. *Surface Science* **1992**, *274*, L541–L545.

(28) LeGoues, F. K.; Horn-Von Hoegen, M.; Copel, M.; Tromp, R. M. Strain-Relief Mechanism in Surfactant-Grown Epitaxial Germanium Films on Si(111). *Phys. Rev. B* **1991**, *44*, 12894–12902.

(29) Horn-von Hoegen, M.; LeGoues, F. K.; Copel, M.; Reuter, M. C.; Tromp, R. M. Defect Self-Annihilation in Surfactant-Mediated Epitaxial Growth. *Phys. Rev. Lett.* **1991**, *67*, 1130–1133.

(30) Fukuma, Y.; Goto, K.; Senba, S.; Miyawaki, S.; Asada, H.; Koyanagi, T.; Sato, H. IV-VI Diluted Magnetic Semiconductor Ge1-xMnxTe Epilayer Grown by Molecular Beam Epitaxy. *Journal of Applied Physics* **2008**, *103*, 053904.

(31) Sławińska, J.; Di Sante, D.; Varotto, S.; Rinaldi, C.; Bertacco, R.; Picozzi, S. Fe/GeTe(111) Heterostructures as an Avenue towards Spintronics Based on Ferroelectric Rashba Semiconductors. *Phys. Rev. B* **2019**, *99*, 075306.

(32) Krizman, G.; Zakusylo, T.; Sajeev, L.; Hajlaoui, M.; Takashiro, T.; Rosmus, M.; Olszowska, N.; Kołodziej, J. J.; Bauer, G.; Caha, O.; Springholz, G. A Novel Ferroelectric Rashba Semiconductor. *Advanced Materials* **2023**, 2310278.

(33) Yashina, L. V.; Püttner, R.; Neudachina, V. S.; Zyubina, T. S.; Shtanov, V. I.; Poygin, M. V. X-Ray Photoelectron Studies of Clean and Oxidized α-GeTe(111) Surfaces. *Journal of Applied Physics* **2008**, *103*, 094909.

(34) Perumal, K. Epitaxial Growth of Ge-Sb-Te Based Phase Change Materials. Ph.D. thesis, Humboldt-Universität zu Berlin, 2013.

(35) Bertoli, S. Toward Spinorbitronics: Investigation of the Ferroelectric Rashba Semiconductor GeTe. Ph.D. thesis, Politecnico di Milano, 2014.

(36) Wang, Z.; Ning, S.; Fujita, T.; Hirata, A.; Chen, M. Unveiling Three-Dimensional Stacking Sequences of 1T Phase MoS $_2$ Monolayers by Electron Diffraction. *ACS Nano* **2016**, *10*, 10308–10316.

(37) Wang, R.; Zhang, W.; Momand, J.; Ronneberger, I.; Boschker, J. E.; Mazzarello, R.; Kooi, B. J.; Riechert, H.; Wuttig, M.; Calarco, R. Formation of Resonant Bonding during Growth of Ultrathin GeTe Films. *NPG Asia Mater* **2017**, *9*, e396–e396.

(38) Jin, Y.; Wang, D.; Qiu, Y.; Zhao, L.-D. Boosting the Thermoelectric Performance of GeTe by Manipulating the Phase Transition Temperature via Sb Doping. *J. Mater. Chem. C* **2021**, *9*, 6484–6490.

Graphical TOC Entry